Article

Two- and Three-Dimensional Smectic Ordering of Single-Handed Helical Polymers

Hisanari Onouchi, Kento Okoshi, Takashi Kajitani, Shin-ichiro Sakurai, Kanji Nagai, Jiro Kumaki, Kiyotaka Onitsuka, and Eiji Yashima

J. Am. Chem. Soc., **2008**, 130 (1), 229-236 • DOI: 10.1021/ja074627u

More About This Article

Additional resources and features associated with this article are available within the HTML version:

- Supporting Information
- Links to the 6 articles that cite this article, as of the time of this article download
- Access to high resolution figures
- Links to articles and content related to this article
- Copyright permission to reproduce figures and/or text from this article

View the Full Text HTML

J|A|C|S
ARTICLES
Published on Web 12/13/2007

Two- and Three-Dimensional Smectic Ordering of Single-Handed Helical Polymers

Hisanari Onouchi,[†] Kento Okoshi,*[,†] Takashi Kajitani,[†] Shin-ichiro Sakurai,[†] Kanji Nagai,[†,‡] Jiro Kumaki,[†] Kiyotaka Onitsuka,[§] and Eiji Yashima*[,†,‡]

Yashima Super-structured Helix Project, Exploratory Research for Advanced Technology (ERATO), Japan Science and Technology Agency (JST), 101 Creation Core Nagoya, 2266-22 Anagahora, Shimoshidami, Moriyama-ku, Nagoya 463-0003, Japan, Department of Molecular Design and Engineering, Graduate School of Engineering, Nagoya University, Chikusa-ku, Nagoya 464-8603, Japan, and The Institute of Scientific and Industrial Research, Osaka University, 8-1 Mihogaoka, Ibaraki, Osaka 567-0047, Japan

Received June 25, 2007; E-mail: kokoshi@yp-jst.jp; yashima@apchem.nagoya-u.ac.jp

Abstract: Rodlike polymers with precisely defined architectures are ideal building blocks for self-assembled structures leading to novel nanometer-scale devices. We found that the living polymerization of a single isocyanide enantiomer bearing an L-alanine pendant with a long *n*-decyl chain simultaneously produced diastereomeric right- and left-handed helices with different molecular weights and narrow molecular weight distributions. Each single-handed, rodlike helical polymer with a controlled length and handedness isolated by a facile solvent fractionation method with acetone self-assembled to form well-defined two- and three-dimensional smectic ordering on the nanometer scale on a substrate and in a liquid crystalline state as evidenced by direct atomic force microscopic observations and X-ray diffraction measurements, respectively.

Introduction

Biological macromolecules, such as DNA and some viruses, possess a well-defined rodlike structure with a one-handed helical sense, which provides access to ideal building blocks for self-assembled nanomaterials and devices. Nucleic acids have been successfully used in the self-assembly of supramolecular arrays through their highly specific binding properties.[1] Some viruses are also known to form smectic liquid crystalline (LC) phases, in which rodlike viruses are packed into layers perpendicular to the direction of their orientation, due to their uniform molecular lengths.[2] Although a bacterial synthetic method has been reported to produce monodisperse polypeptides with a state-of-the-art control of the molecular lengths and structures,[3] it remains a great challenge to control those of the artificial helical polymers to such an extent in a conventional synthetic way,[4] not only to mimic the structures of biological helices but also to develop novel functions.[5]

Fully synthetic optically active helical polymers have been prepared either by the polymerization of optically active monomers, such as isocyanates,[5g] silanes,[5e] acetylenes,[5c] or by the helix-sense selective polymerization of achiral methacrylates,[5f] isocyanides,[5d,6] and carbodiimides[7] bearing bulky substituents by chiral catalysts or initiators. The former polymerization produces dynamic helical polymers composed of interconverting right- and left-handed helical segments separated by rarely occurring helical reversals,[5c,e,g] and the latter static helical polymers whose helical conformations are locked during the polymerization under kinetic control.[5f,6]

In earlier studies, we reported the conventional polymerization of an enantiomerically pure phenyl isocyanide bearing an L-alanine pendant with a long *n*-decyl chain through an amide linkage (L-**1**) with $NiCl_2$ as a catalyst, which produced a rodlike static helical polyisocyanide with a broad molecular weight

[†] ERATO, JST.
[‡] Graduate School of Engineering, Nagoya University.
[§] The Institute of Scientific and Industrial Research, Osaka University.

(1) (a) Seeman, N. C. *Int. J. Nanotechnol.* **2005**, *2*, 348−370. (b) Winfree, E.; Liu, F.; Wenzler, L. A.; Seeman, N. C. *Nature* **1998**, *394*, 539−544.
(2) (a) Lee, S.-W.; Wood, B. M.; Belcher, A. M. *Langmuir* **2003**, *19*, 1592−1598. (b) Lee, S.-W.; Mao, C.; Flynn, C. E.; Belcher, A. M. *Science* **2002**, *296*, 892−895. (c) Dogic, Z.; Faden, S. *Phys. Rev. Lett.* **1997**, *78*, 2417−2420. (d) Wen, X.; Meyer, R. B.; Casper, D. L. D. *Phys. Rev. Lett.* **1989**, *63*, 2760−2763.
(3) (a) Yu, S. M.; Conticello, V. P.; Zhang, G.; Kayser, C.; Fournier, M. J.; Mason, T. L.; Tirrell, D. A. *Nature* **1997**, *389*, 167−170. (b) Zhang, G.; Fournier, M. J.; Mason, T. L.; Tirrell, D. A. *Macromolecules* **1992**, *25*, 3601−3603.
(4) (a) Kim, K. T.; Park, C.; Kim, C.; Winnik, M. A.; Manners, I. *Chem. Commun.* **2006**, 1372−1374. (b) Okoshi, K.; Sano, N.; Suzaki, G.; Tokita, M.; Magoshi, J.; Watanabe, J. *Jpn. J. Appl. Phys.* **2002**, *41*, L720−L722. (c) Okoshi, K.; Kamee, H.; Suzaki, G.; Tokita, M.; Fujiki, M.; Watanabe, J. *Macromolecules* **2002**, *35*, 4556−4559.
(5) (a) Yashima, E.; Maeda, K. In *Foldamers: Structure, Properties, and Applications*; Hecht, S., Huc, I., Eds.; Wiley: Weinheim, 2007; pp 331−366. (b) Hoeben, F. J. M.; Jonkheijm, P.; Meijer, E. W.; Schenning, P. H. J. *Chem. Rev.* **2005**, *105*, 1491−1546. (c) Yashima, E.; Maeda, K.; Nishimura, T. *Chem.*−Eur. J. **2004**, *10*, 42−51. (d) Elemans, J. A. A. W.; Rowan, A. E.; Nolte, R. J. M. *J. Mater. Chem.* **2003**, *13*, 2661−2670. (e) Fujiki, M. *Macromol. Rapid Commun.* **2001**, *22*, 539−563. (f) Nakano, T.; Okamoto, Y. *Chem. Rev.* **2001**, *101*, 4013−4038. (g) Green, M. M.; Park, J.-W.; Sato, T.; Teramoto, A.; Lifson, S.; Selinger, R. L. B.; Selinger, J. V. *Angew. Chem., Int. Ed.* **1999**, *38*, 3138−3154.
(6) (a) Amabilino, D. B.; Serrano, J.-L.; Sierra, T.; Veciana, J. *J. Polym. Sci., Part A: Polym. Chem.* **2006**, *44*, 3161−3174. (b) Suginome, M.; Ito, Y. *Adv. Polym. Sci.* **2004**, *17*, 77−136. (c) Cornelissen, J. J. L. M.; Rowan, A. E.; Nolte, R. J. M.; Sommerdijk, N. A. J. M. *Chem. Rev.* **2001**, *101*, 4039−4070.
(7) (a) Tang, H.-Z.; Boyle, P. D.; Novak, B. M. *J. Am. Chem. Soc.* **2005**, *127*, 2136−2142. (b) Tian, G.; Lu, Y.; Novak, B. M. *J. Am. Chem. Soc.* **2004**, *126*, 4082−4083.

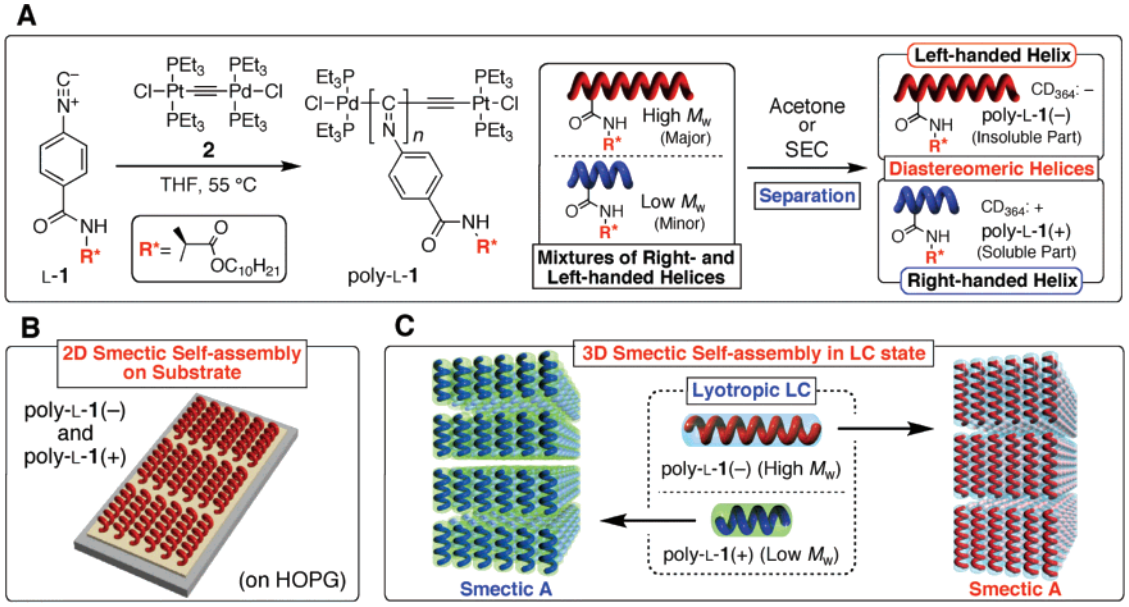

Figure 1. Two- and three-dimensional smectic ordering of helical polymers. (A) Schematic illustration of the helix-sense selective living polymerization of L-**1** with μ-ethynediyl Pt−Pd complex (**2**), yielding a mixture of diastereomeric, right- and left-handed helical poly-L-**1**'s with different molecular weights and a narrow MWD, which can be further separated into each single-handed helical poly-L-**1**. Two-dimensional (B) and 3D (C) smectic ordering of the one-handed helical poly-L-**1**'s on substrate and in LC state.

distribution (MWD), thus forming a lyotropic cholesteric LC phase in concentrated solutions, whose helical sense was roughly dictated by the polymerization solvent and temperature.[8] Nolte and co-workers prepared a series of peptide-bound helical polyisocyanides stabilized by intramolecular hydrogen bonds from optically pure isocyanopeptides using nickel or acid catalysts, which resulted in the formation of a similar cholesteric LC phase due to its polydisperse nature.[5d,6c,9] Herein we show that the living polymerization of L-**1** with the μ-ethynediyl Pt−Pd catalyst (**2**) simultaneously creates both almost completely right- and left-handed helical polyisocyanides (poly-L-**1**) with a different molecular weight and sufficiently narrow MWD (Figure 1A). Each helical poly-L-**1** can be separated in a facile way and exhibits well-defined two (2D)- and three-dimensional (3D) smectic ordering on a substrate and in an LC state, as directly observed by atomic force microscopy (AFM) and revealed by X-ray diffraction (XRD), respectively (B and C of Figure 1).

Results and Discussion

The polymerization of D- or L-**1** with **2** ([**1**]/[**2**] = 50, 100, or 200 (mol/mol)) as the initiator, which is known to promote the living polymerization of aryl isocyanide,[10] was conducted in tetrahydrofuran (THF) at 55 °C and quantitatively produced rodlike helical polyisocyanides ([D- or L-**1**]/[**2**] = 100 for poly-D-**1** or poly-L-**1**, [L-**1**]/[**2**] = 50 for poly-L-$\mathbf{1}_{50}$, and [L-**1**]/[**2**] = 200 for poly-L-$\mathbf{1}_{200}$). Size exclusion chromatography (SEC) of poly-L-**1** detected by UV (254 nm) and circular dichroism (CD) (364 nm) revealed a bimodal distribution with a sharp main peak together with a small peak in the lower molecular weight (M_w) region whose CD signs were opposite, negative, and positive, respectively (Figure 2A), suggesting a mixture of right- and left-handed helices with different M_w's. We found that each helical poly-L-**1** could be easily separated by fractionation with acetone into acetone-insoluble and -soluble fractions which showed unimodal chromatograms with negative and positive CD signs at 364 nm for the high-M_w poly-L-**1**(−) and low-M_w poly-L-**1**(+), respectively (B and C of Figure 2). The CD spectra of poly-L-**1**(−) and poly-L-**1**(+) in the $n-\pi^*$ transition of the imino chromophore regions of the polymer backbones (280−480 nm) as well as in the pendant aromatic regions (240−280 nm)[10,11] are almost mirror images of each other with a greater intensity than the intensity of those before the fractionation (Figure 2D). These results indicate that the as-prepared poly-L-**1** is indeed a mixture of right- and left-handed helices.[12] We note that they are not enantiomers, but diastereomers with a

(8) Kajitani, T.; Okoshi, K.; Sakurai, S.-i.; Kumaki, J.; Yashima, E. *J. Am. Chem. Soc.* **2006**, *128*, 708−709.
(9) (a) Metselaar, G. A.; Adams, P. J. H. M.; Nolte, R. J. M.; Cornelissen, J. J. L. M.; Rowan, A. E. *Chem. Eur. J.* **2007**, *13*, 950−960. (b) Metselaar, G. A.; Wezenberg, S. J.; Cornelissen, J. J. L. M.; Nolte, R. J. M.; Rowan, A. E. *J. Polym. Sci., Part A: Polym. Chem.* **2007**, *45*, 981−988. (c) Metselaar, G. A.; Cornelissen, J. J. L. M.; Rowan, A. E.; Nolte, R. J. M. *Angew. Chem., Int. Ed.* **2005**, *44*, 1990−1993. (d) Cornelissen, J. J. L. M.; Graswinckel, W. S.; Rowan, A. E.; Sommerdijk, N. A. J. M.; Nolte, R. J. M. *J. Polym. Sci., Part A: Polym. Chem.* **2003**, *41*, 1725−1736. (e) Cornelissen, J. J. L. M.; Sommerdijk, N. A. J. M.; Nolte, R. J. M. *Macromol. Chem. Phys.* **2002**, *203*, 1625−1630. (f) Cornelissen, J. J. L. M.; Donners, J. J. J. M.; de Gelder, R.; Graswinckel, W. S.; Metselaar, G. A.; Rowan, A. E.; Sommerdijk, N. A. J. M.; Nolte, R. J. M. *Science* **2001**, *293*, 676−680.
(10) (a) Takei, F.; Hayashi, H.; Onitsuka, K.; Kobayashi, N.; Takahashi, S. *Angew. Chem., Int. Ed.* **2001**, *40*, 4092−4094. (b) Onitsuka, K.; Joh, T.; Takahashi, S. *Chem. Eur. J.* **2000**, *6*, 983−993. (c) Onitsuka, K.; Joh, T.; Takahashi, S. *Angew. Chem., Int. Ed. Engl.* **1992**, *31*, 851−852.
(11) (a) Hase, Y.; Mitsutsuji, Y.; Ishikawa, M.; Maeda, K.; Okoshi, K.; Yashima, E. *Chem. Asian J.* **2007**, *2*, 755−763. (b) Ishikawa, M.; Maeda, K.; Mitsutsuji, Y.; Yashima, E. *J. Am. Chem. Soc.* **2004**, *126*, 732−733.
(12) The difference in the M_w's of poly-L-**1**(−) and poly-L-**1**(+) can be explained on the basis of the difference in propagation rates of the two growing species, giving high- and low-M_w polymers, respectively. Plots of the number-average molecular weight (M_n) of left-handed helical poly-L-**1**(−) and right-handed helical poly-L-**1**(+) versus feed molar ratio of the monomer L-**1** to the initiator (**2**) ([L-**1**]/[**2**]) gave an almost linear correlation (Figure S10), which is indicative of a mechanism in which diastereomeric oligomers of L-**1** with both helical senses are formed during the initial stage of polymerization and one of the two appears to propagate rapidly over the other, producing right- and left-handed helical poly-L-**1**'s with different M_w's. The reason why diastereomeric oligomers with both helical senses are formed during the initial stage of polymerization of L-**1** is not clear at present, but it may be correlated with the previous observations that the conventional polymerization of L-**1** with $NiCl_2$ as a catalyst produced poly-L-**1**'s, whose helical senses were considerably influenced by the polymerization solvent and temperature.[8]

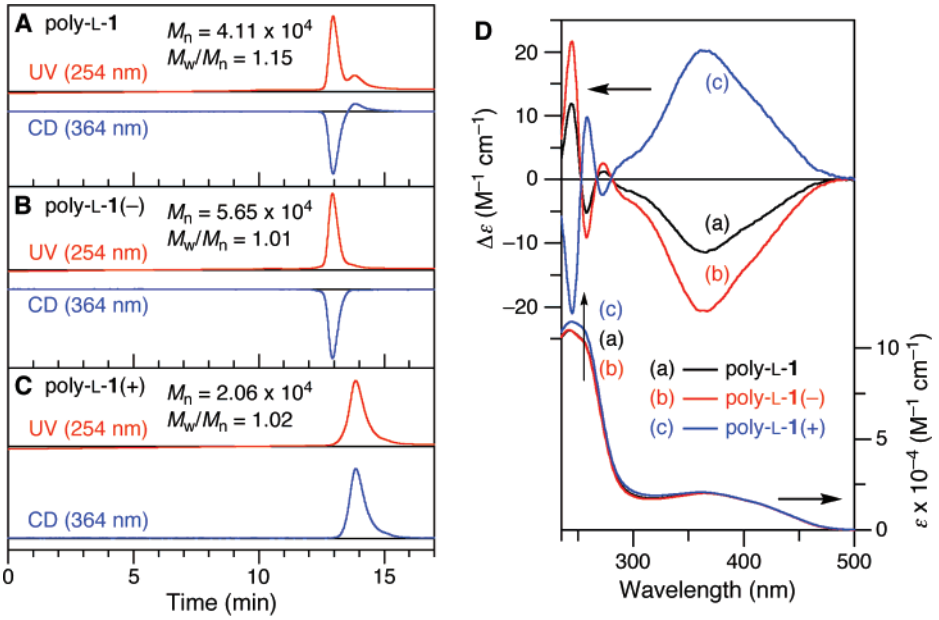

Figure 2. Right- and left-handed helical poly-L-**1**. (A−C) SEC chromatograms of the as-prepared poly-L-**1** (A) and the isolated acetone-insoluble poly-L-**1**(−) (B) and acetone-soluble poly-L-**1**(+) (C) using UV (red lines) and CD (blue lines) detectors in THF containing 0.1 wt % tetra-*n*-butylammonium bromide. (D) CD and absorption spectra of poly-L-**1** (a), poly-L-**1**(−) (b), and poly-L-**1**(+) (c) (0.2 mg/mL) in chloroform at 25 °C. The number-average molecular weight (M_n) and its distribution (M_w/M_n) of each polymer as determined by SEC coupled with a multi-angle light-scattering (MALS) detector (SEC-MALS) measurements are also shown in A−C.

different solubility in acetone, and thereby, they can be separated. This conclusion is supported by the fact that even a mixture of poly-L-**1**(−) and poly-L-**1**(+) with comparable M_w's could be also separated into each helix using acetone. In the same way, the as-prepared poly-D-**1** can be fractionated using acetone into right- and left-handed helical poly-D-**1**'s with different M_w's and a narrow MWD (Figure S1).

Polyisocyanides bearing a bulky substituent have been considered to have a 4 units per turn (4/1) helical conformation even in solution, although their exact helical structures have not yet been elucidated[6c,9] probably because of difficulty in obtaining a uniaxially oriented polymer film suitable for XRD measurements. The poly-L-**1**(−) and poly-L-**1**(+) are rigid-rod helical polymers and exhibit a lyotropic smectic LC phase (see below), which enables us to determine their structures by XRD and AFM. Figure 3A shows a wide-angle X-ray diffraction (WAXD) pattern of an oriented poly-L-**1**(−) film prepared from a concentrated LC benzene solution in an electric field; for a WAXD pattern of poly-L-**1**(+), see Figure S2. The electric field-induced alignment of poly-L-**1** molecules evidenced a large dipole moment of poly-L-**1** along its helical axis, that is all the intramolecularly hydrogen-bonded N−H and C═O groups are oriented in one direction so as to accumulate the large dipole moment as observed in the typical α-helical polypeptides.[13] The WAXD patterns of the films of poly-L-**1**(−) and poly-L-**1**(+) show diffuse, but apparent meridional and equatorial reflections, suggesting that they possess a similar helical structure; a 15 units per 4 turns (15/4) helix with a hexagonal lattice (Table S1) which satisfies the density requirements.[14] Optimized molecular structures for the 15/4 helices of the left-handed helical poly-L-**1**(−) model (158-mer) and right-handed helical poly-L-**1**(+) model (58-mer), based on the absolute molecular weights (M_n = 5.65 × 10^4 and 2.06 × 10^4, respectively) calculated by the SEC measurements coupled with a multi-angle light scattering (MALS) detector, are illustrated in B and C of Figure 3, respectively. The detailed structures (11-mer) taken from Figure 3B are also shown in D and E of Figure 3 (see also Supporting Information). The polymer models appear to have four sets of hydrogen-bonded helical arrays linking *n* and (*n* + 4) pendants with the quarter helical pitch and chain length of 1.31 and 13.7 nm, and 1.31 and 5.1 nm, for poly-L-**1**(−) and poly-L-**1**(+), respectively. IR spectra suggested the formation of such intramolecular hydrogen bonds between the pendant amide residues of poly-L-**1**(−) and poly-L-**1**(+) (Figure S3). The equivalent interpendant hydrogen bonds were observed in the crystalline structure of L-**1**, in which the amide linkage was oblique to the phenyl ring (ca. 30°) (Figure S4). Helical polyisocyanides stabilized by intramolecular hydrogen bonds have been reported by Nolte and co-workers.[6c,9]

Parts F and G of Figure 3 show high-resolution AFM images of poly-L-**1**(−) and poly-L-**1**(+), respectively, cast from a benzene solution (0.015 mg/mL) on highly oriented pyrolytic graphite (HOPG) followed by benzene vapor exposure at ca. 20 °C for 12 h.[8,15,16] The poly-L-**1** self-assembles into well-defined 2D helix bundles with a controlled molecular length,[17] most of which are clearly resolved into individual left- (Figure 3F) and right-handed (Figure 3G) helices packed parallel to each other. The AFM images as well as those of larger areas confirmed the helical pitch, helical sense, helix-sense excess,

(13) Wada, A. *Adv. Biophys.* **1976**, *9*, 1−63.

(14) The observed densities of the poly-L-**1**(−) and poly-L-**1**(+) films were 1.0739 and 1.0624 g/cm^3, respectively, measured by the standard flotation method in an aqueous NaCl solution containing a small amount of a surfactant at ambient temperature (20−25 °C). The 15/4 helices of poly-L-**1**(−) and poly-L-**1**(+) in the hexagonal lattices require the densities of 1.102 and 1.089 g/cm^3, respectively, which are in good agreement with the observed values. When the number of repeating units per fiber period is assumed to be other than 15, the calculated densities were considerably different from the observed densities. For more details, see Supporting Information.

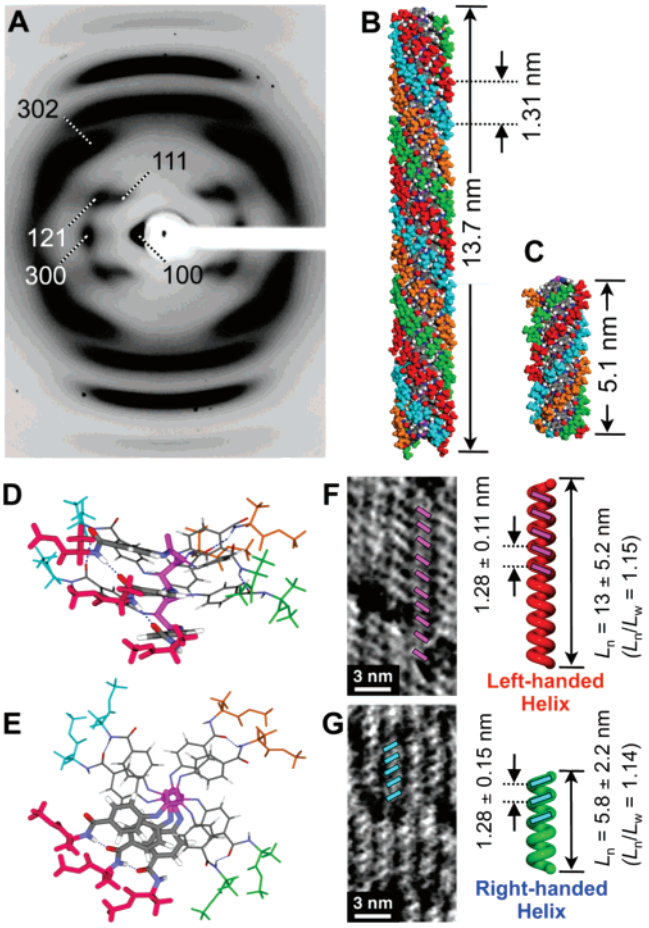

Figure 3. Structures of helical poly-L-**1**'s. (A) WAXD pattern of an oriented poly-L-**1**(−) film prepared from a concentrated LC benzene solution (ca. 15 wt %). The reflections were indexed with a hexagonal lattice; $a = 26.78$ Å and $c = 13.05$ Å, suggesting a 15 units per 4 turns (15/4) helical structure. (B and C) Optimized 15/4 helical structures of poly-L-**1**(−) (B, 158-mer) and poly-L-**1**(+) (C, 58-mer) on the basis of WAXD structural analyses followed by molecular mechanics calculations (see Supporting Information). Each structure is represented by space-filling models, and four sets of hydrogen-bonded helical arrays (n and $n + 4$) of the pendants are shown in different colors for clarity. (D and E) The detailed structure of poly-L-**1**(−) (11-mer) taken from (B) is also shown by a stick model in D (side view) and E (top view). In these models (B−E), the pendant decyl ester groups of poly-L-**1**'s are replaced by the methyl groups for clarity. (F and G) AFM phase images of poly-L-**1**(−) (F) and poly-L-**1**(+) (G) on HOPG (scale = 10 × 20 nm). Schematic representations of the left-handed helical poly-L-**1**(−) and right-handed helical poly-L-**1**(+) structures with periodic oblique stripes (pink and blue lines, respectively) which denote a one-handed helical array of the pendants, are also shown (right). On the basis of an evaluation of ca. 100 molecules, the number-average molecular length (L_n) and the length distribution (L_w/L_n) were estimated.

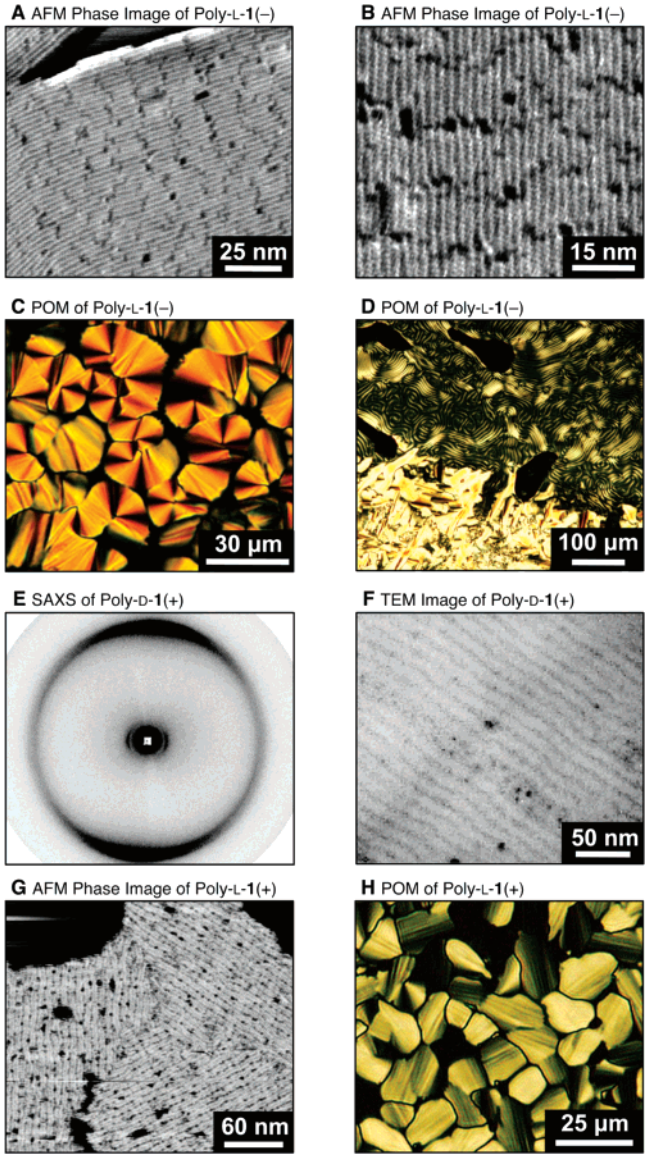

Figure 4. Two-dimensional and 3D smectic ordering of poly-L-**1**. (A and B) AFM phase images of 2D self-assembled poly-L-**1**(−) on HOPG. (C) Polarized optical micrograph (POM) of poly-L-**1**(−) in ca. 15 wt % chloroform solution taken at ambient temperature (20−25 °C). (D) A lyotropic smectic−cholesteric phase transition of poly-L-**1**(−) in chloroform placed between a glass plate and a cover glass, driven by gradual solvent evaporation from the edge (lower part). (E) SR-SAXS pattern of a poly-D-**1**(+) cast film prepared from a concentrated smectic LC solution aligned in the magnetic field, taken perpendicular to the direction of the magnetic field. (F) Bright-field TEM image of the banding with a repeat distance of ca. 14 nm in a poly-D-**1**(+) cast film (ca. 30 nm thickness) ultramicrotomed and stained in RuO_4 vapor. (G) AFM phase image of 2D self-assembled poly-L-**1**(+) on HOPG. (H) POM of poly-L-**1**(+) in ca. 15 wt % chloroform solution taken at ambient temperature (20−25 °C).

and molecular arrangement of poly-L-**1**'s. The periodic oblique stripes observed in each helical chain, that originated from a one-handed helical array of the pendants, were tilted counterclockwise or clockwise at −55° and +62°, for poly-L-**1**(−) and poly-L-**1**(+), respectively, with respect to the main-chain axis. This remarkable 2D mirror-image relationship suggests that the poly-L-**1**(−) and poly-L-**1**(+) molecules most likely consist of left- and right-handed helical structures with a helical pitch of 1.28 ± 0.11 and 1.28 ± 0.15, respectively, as estimated from the average distance between each stripe (F and G of Figure 3). The helical pitches estimated by AFM are almost identical to the quarter helical pitches of the pendant arrangements as determined by the WAXD (1.31 nm). In addition, on the basis of an evaluation of about 1000 helical blocks, the helix-sense

(15) This method is very useful for constructing highly ordered 2D helix-bundles for helical polyacetylenes and polyisocyanides on HOPG, and their helical structures were visualized by AFM.[8,16]
(16) Sakurai, S.-i.; Okoshi, K.; Kumaki, J.; Yashima, E. *Angew. Chem., Int. Ed.* **2006**, *45*, 1245−1248.
(17) On the basis of an evaluation of about 100 individual polymer chains separated from one another, the number-average molecular length (L_n) and the length distribution (L_w/L_n) of poly-L-**1**(−) and poly-L-**1**(+) were estimated to be 13 ± 5.2 nm and 1.15 and 5.8 ± 2.2 nm and 1.14, respectively. The estimated chain lengths by AFM almost perfectly coincide with those estimated by the SEC-MALS (B and C of Figure 3).

Scheme 1

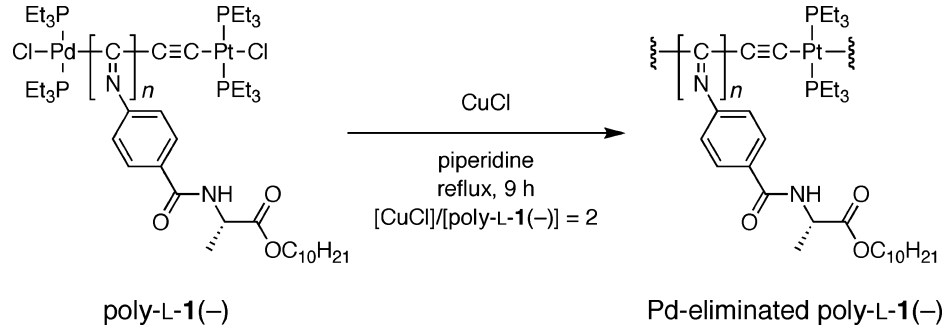

poly-L-**1**(–) Pd-eliminated poly-L-**1**(–)

excesses of poly-L-**1**(−) and poly-L-**1**(+) were estimated to be 98.7 and 96.5%, respectively.[18]

Further AFM observations of the bundle structures of the poly-L-**1**(−) on HOPG revealed a 2D smecticlike self-assembly of the polymer chains with a controlled spacing (A and B of Figure 4). The layer structure is nearly perpendicular to the direction of the polymer chains. The average layer spacing of the 2D smecticlike self-assembled polymer chains increased with the increasing M_w or rod length of the polymers: 5.8, 13, and 28 nm for poly-L-**1**(+), poly-L-**1**(−), and poly-L-$\mathbf{1}_{200}$(−), respectively (Figure S6).[19] We note that the 2D smecticlike self-assemblies of the polymer chains simultaneously guide the 1D arrays of the Pt and Pd metals bonded at the polymer ends, which may also be used for fabricating nanostructured materials. Rodlike helical poly-L-**1**'s with a narrow MWD appear to be indispensable for the 2D smectic ordering on a substrate. Considerably clear layered images of smectic LC small molecules on substrates have also been observed by scanning tunneling microscopy, but controllable layer spacings are limited to within a few nanometers.[20]

Polarized optical microscopy of a concentrated solution of poly-L-**1**(−) in chloroform (ca. 15 wt %) demonstrated that the polymer forms a typical smectic phase (smectic A) as evidenced by its indisputably clear fan-shaped texture (Figure 4C). A cholesteric−smectic phase transition could be also observed in a concentration gradient (Figure 4D). To the best of our knowledge, this is the first microscopic observation of a lyotropic cholesteric−smectic phase transition upon dilution of a helical polymer based on the main-chain stiffness. The decisive evidence of the smectic layer structure was obtained from synchrotron radiation small-angle X-ray diffraction (SR-SAXS) of oriented poly-**1** films prepared from a concentrated smectic LC chloroform solution in a magnetic field (11.75 T for 1 day) by slow evaporation.[21] SR-SAXS of a magnetically oriented poly-D-**1**(+) film showed a sharp reflection with a spacing of 14.3 nm in a meridional direction perpendicular to the outer broad reflection of 2.32 nm being attributable to the lateral packing of the polymer (Figure 4E). The spacing of 14.3 nm is almost identical to that determined by AFM.[22] The observed spacing by SR-SAXS becomes longer when the molecular length or rod length of the poly-**1**'s is longer and the layer spacings determined by SR-SAXS and AFM are in good agreement to each other (Figures S8 and S9). A theoretical study predicted that the smectic ordering is not favored for rodlike polymers with a broad MWD, since the rods of different lengths do not pack into layers as effectively as the rod of the same length.[23] In fact, poly-**1**'s with MWDs over 1.15 no longer showed any sign of smectic phases. Transmission electron microscopy (TEM) of an ultramicrotomed cast film of a smectic LC of poly-D-**1**(+) showed a banded texture (Figure 4F) with a repeat distance of ca. 14 nm corresponding to its smectic layer repeat as observed by SR-SAXS measurements,[22] even though the banding repeat distance depends on the local contact angle between the sample and the diamond knife.[24] AFM observations of poly-L-**1**(+) on HOPG also revealed a 2D smecticlike assembly of the polymer chains with an average layer spacing of 5.8 ± 2.2 nm (Figure 4G), and the polarized optical micrograph of poly-L-**1**(+) showed a similar fan-shaped texture in a 15 wt % chloroform solution (Figure 4H), offering convincing proof for a smectic ordering.

Conclusions

In summary, we have demonstrated that the present helix-sense selective living polymerization with the μ-ethynediyl Pt−Pd catalyst unprecedentedly produces both right- and left-handed helical, rigid-rod polyisocyanides at once with precisely defined architectures including the molecular length, its distribution, and handedness as well, which can be further separated into each helix in a facile way. More importantly, these helical polyisocyanides are proven to be ideal building blocks for 2D and 3D smectic arrangements on a substrate, in solution and the solid

(18) In the same way, the L_n, L_w/L_n, helical sense, and helical pitch of poly-L-$\mathbf{1}_{200}$(−) and poly-D-**1**(+) can be estimated from the high-resolution AFM images (Figure S5).

(19) We preliminarily measured high-resolution AFM images of the as-prepared poly-L-**1** (a mixture of high-molecular weight poly-L-**1**(−) and low-molecular weight poly-L-**1**(+)) cast from a benzene solution on HOPG. We anticipated a spontaneous diastereomeric domain formation. However, as shown in Figure S11, 2D smecticlike layered domains composed of either a right- or left-handed helical poly-L-**1** could not be clearly observed. It seems likely that the molecular length may play a dominant role in such a 2D smecticlike layer formation. Apparently, a further thorough study is necessary to explore a possible spontaneous domain formation.

(20) (a) Hara, M.; Iwakabe, Y.; Toguchi, K.; Sasabe, H.; Garito, A. F.; Yamada, A. *Nature* **1990**, *344*, 228−230. (b) Smith, D. P. E.; Hörber, H.; Gerber, Ch.; Binnig, G. *Science* **1989**, *245*, 43−45. For reviews: (c) De Feyter, S.; De Schryver, F. C. *Chem. Soc. Rev.* **2003**, *32*, 139−150. (d) Pérez-García, L.; Amabilino, D. B. *Chem. Soc. Rev.* **2002**, *31*, 342−356. (e) Giancarlo, L. C.; Flynn, G. W. *Acc. Chem. Res.* **2000**, *33*, 491−501.

(21) Poly-D-**1**(+) was treated with CuCl in piperidine to eliminate the terminal Pd residues prior to the SR-SAXS measurements, since the smectic layer reflections could not be observed for the magnetic-oriented polymers bearing the terminal Pd residues prepared under identical conditions; the reason is not clear, but probably due to the high atomic scattering factor of the Pd metals at the polymer ends (for more details, see Experimental Section and Supporting Information).

(22) Two-dimensional smecticlike assemblies of the polymer chains with a controlled spacing were also observed in AFM images of poly-D-**1**(+) on HOPG (Figure S7). The average layer spacing 14 nm is consistent with that determined by SR-SAXS and TEM.

(23) Bates, M. A.; Frenkel, D. J. *J. Chem. Phys.* **1998**, *109*, 6193−6199.

(24) He, S.-J.; Lee, C.; Gido, S. P.; Yu, S. M.; Tirrell, D. A. *Macromolecules* **1998**, *31*, 9387−9389.

state, assisted by four sets of intramolecular hydrogen-bonding helical arrays of the pendants. In addition, the helical structures of the polyisocyanides including the helical pitch and handedness were for the first time determined by high-resolution AFM observations combined with X-ray diffraction measurements. We anticipate that the helical polyisocyanides bearing Pt and Pd at the ends may also be used as a novel template to organize one-dimensional arrays of inorganic materials on the nanoscale by modification of the catalyst, which may be applicable to the next-generation optical, electric, and magnetic devices.

Experimental Section

Instruments. The NMR spectra were measured using a Varian AS500 spectrometer (Varian, Palo Alto, CA) operating at 500 MHz for ^{1}H and 125 MHz for ^{13}C, using TMS as the internal standard. The IR spectra were recorded using a JASCO FT/IR-680 spectrometer (JASCO, Tokyo, Japan). The absorption and CD spectra were obtained in a 1.0-mm quartz cell using a JASCO V570 spectrophotometer and a JASCO J820 spectropolarimeter, respectively. The polymer concentration was calculated on the basis of the monomer units and was 0.2 mg/mL. The optical rotations were measured in a 2-cm quartz cell on a JASCO P-1030 polarimeter. SEC was performed using a JASCO PU-2080 liquid chromatograph equipped with UV−visible (JASCO UV-2070) and CD (JASCO CD-2095) detectors. Two Tosoh TSKgel MultiporeH$_{XL}$-M SEC columns (Tosoh, Tokyo, Japan) were connected in series, and THF containing 0.1 wt % tetra-*n*-butylammonium bromide was used as the eluent at the flow rate of 1.0 mL/min. The molecular weight calibration curve was obtained with standard polystyrenes (Tosoh). The WAXD measurements were carried out using a Rigaku RINT RAPID-R X-ray diffractometer (Rigaku, Tokyo, Japan) with a rotating-anode generator and graphite monochromated CuKα radiation (0.15418 nm) focused through a 0.3 mm pinhole collimator, which was supplied at a 45 kV voltage and a 60 mA current, equipped with a curved imaging plate having a specimen-to-plate distance of 120.0 mm. The X-ray photographs were taken at ambient temperature (20−25 °C) from the edge-view position with a beam parallel to the film surface. The SEC-MALS measurements were performed using an HLC-8220 GPC system (Tosoh) equipped with a differential refractometer coupled to a DAWN-EOS MALS device equipped with a semiconductor laser (λ = 690 nm) (Wyatt Technology, Santa Barbara, CA) operated at 25 °C using two TSKgel Multipore H$_{XL}$-M columns (Tosoh) in series. The scattered light intensities were measured by 18 light-scattering detectors at different angles. The differential refractive index increment, d*n*/d*c*, of the polymer with respect to the mobile phase at 25 °C was also measured by an Optilab rEX interferometric refractometer (Wyatt Technology). The AFM measurements were performed using a Nanoscope IIIa or Nanoscope IV microscope (Veeco Instruments, Santa Barbara, CA) in air at ambient temperature (ca. 25 °C) with standard silicon cantilevers (NCH, NanoWorld, Neufchâtel, Switzerland) in the tapping mode. The polarizing optical microscopic observations were carried out with an E600POL polarizing optical microscope (Nikon, Tokyo, Japan) equipped with a DS-5M CCD camera (Nikon) connected to a DS-L1 control unit (Nikon). The sample solution was placed on a glass plate with a cover glass to develop the planar structure before observation of the microscopic texture at ambient temperature (20−25 °C). The SR-SAXS measurements were performed at the Institute of Materials Structure Science, Tsukuba, Japan (Photon Factory), with small-angle X-ray equipment installed on a beam line, BL15A, with the approval of the Photon Factory Program Advisory Committee (No. 2006G293). The wavelength of the incident X-ray beam was 0.1508 nm. X-ray photographs were taken using a flat imaging plate placed 2400 mm from the sample position at ambient temperature (20−25 °C). The TEM observations were performed using a Hitachi H-800 instrument operated at 100 kV. The sample was prepared by casting a concentrated solution of poly-D-**1**(+) in chloroform showing an LC phase on a poly(tetrafluoroethylene) (PTFE) petri dish. After gradual evaporation of the solvent, the cast film was annealed at 170 °C for 2 days. The obtained cast film was embedded in epoxy resin (ThreeBond 2082C) and ultramicrotomed perpendicular to the cast film surface. The thin film (ca. 30 nm thick) was then stained by RuO_4 vapor for 7 min before the TEM observations.

Materials. Anhydrous chloroform and toluene (water content <50 ppm) were purchased from Aldrich and stored under dry nitrogen. THF was dried over sodium benzophenone ketyl, distilled onto $LiAlH_4$ under nitrogen, and distilled under high vacuum just before use. The 4-isocyanobenzoyl-L- and D-alanine decyl esters (L-**1** and D-**1**)[8] and the μ-ethynediyl Pt−Pd complex (**2**)[10] were prepared as previously reported.

Polymerization. The polymerization of L-**1** was carried out in a dry glass ampule under a dry nitrogen atmosphere using **2** as the catalyst in dry THF. A typical experimental procedure is described below. Monomer L-**1** (300 mg, 0.84 mmol) was placed in a dry ampule, which was then evacuated on a vacuum line and flushed with dry nitrogen. After this evacuation−flush procedure had been repeated three times, a three-way stopcock was attached to the ampule, and dry THF (3.4 mL) was added by a syringe. To this was added a solution of **2** in THF (10 μM, 0.81 mL) at ambient temperature. The concentrations of L-**1** and **2** were 0.2 and 0.002 M, respectively ([**1**]/[**2**] = 100). The mixture was then stirred under a dry nitrogen atmosphere and heated to 55 °C. After 20 h, the resulting polymer (poly-L-**1**) was precipitated in a large amount of methanol, collected by centrifugation, and dried in vacuo at room temperature overnight (286 mg, 96% yield).

Spectroscopic data of poly-L-1: IR (KBr, cm^{-1}): 3277 (ν_{N-H}), 1750 ($\nu_{C=O}$ ester), 1635 (amide I), 1535 (amide II); ^{1}H NMR ($CDCl_3$, 55 °C): δ 0.87 (broad, CH_3, 3H), 1.26 (broad, CH_2, 14H), 1.53 (broad, CH_3 and CH_2, 5H), 4.09 (broad, CH_2, 2H), 4.51 (broad, CH, 1H), 4.8−7.7 (broad, aromatic, 4H), 7.9−9.0 (broad, NH, 1H); $[\alpha]^{25}_D$ −995° (*c* 0.1, chloroform); Anal. Calcd (%) for $(C_{21}H_{30}N_2O_3)_n$: C, 70.36; H, 8.44; N, 7.81. Found: C, 70.23; H, 8.56; N, 7.68.

Fractionation. The obtained poly-L-**1** (70.8 mg) was suspended in 30 mL of acetone, and the mixture was stirred at ambient temperature for 3 h. After filtration, the filtrate was evaporated to dryness under reduced pressure, giving poly-L-**1**(+) (10.0 mg, 14%). The acetone-insoluble polymer was dissolved in a small amount of chloroform, the solution was precipitated in a large amount of acetone, and the precipitate was then collected by filtration. After this procedure was repeated again, the poly-L-**1**(−) was obtained (44.5 mg, 63%).

Spectroscopic data of poly-L-1(+): IR (KBr, cm^{-1}): 3279 (ν_{N-H}), 1750 ($\nu_{C=O}$ ester), 1635 (amide I), 1535 (amide II); ^{1}H NMR ($CDCl_3$, 55 °C): δ 0.90 (broad, CH_3, 3H), 1.29 (broad, CH_2, 14H), 1.62 (broad, CH_3 and CH_2, 5H), 4.11 (broad, CH_2, 2H), 4.51 (broad, CH, 1H), 4.9−7.7 (broad, aromatic, 4H), 8.3−9.0 (broad, NH, 1H); $[\alpha]^{25}_D$ +1530° (*c* 0.05, chloroform). Anal. Calcd (%) for $(C_{21}H_{30}N_2O_3)_n$: C, 70.36; H, 8.44; N, 7.81. Found: C, 70.18; H, 8.44; N, 7.78.

Spectroscopic data of poly-L-1(−): IR (KBr, cm^{-1}): 3282 (ν_{N-H}), 1750 ($\nu_{C=O}$ ester), 1635 (amide I), 1535 (amide II); ^{1}H NMR ($CDCl_3$, 55 °C): δ 0.87 (broad, CH_3, 3H), 1.25 (broad, CH_2, 14H), 1.53 (broad, CH_3 and CH_2, 5H), 4.09 (broad, CH_2, 2H), 4.51 (broad, CH, 1H), 4.8−7.7 (broad, aromatic, 4H), 7.9−8.9 (broad, NH, 1H); $[\alpha]^{25}_D$ −1615° (*c* 0.1, chloroform). Anal. Calcd (%) for $(C_{21}H_{30}N_2O_3)_n$: C, 70.36; H, 8.44; N, 7.81. Found: C, 70.35; H, 8.36; N, 7.64.

Poly-D-**1** was also prepared by the polymerization of D-**1** with **2** ([**1**]/[**2**] = 100) in the same way as described above, and the acetone-insoluble part (poly-D-**1**(+)) was obtained by fractionation with acetone.

Spectroscopic data of poly-D-1: IR (KBr, cm^{-1}): 3276 (ν_{N-H}), 1751 ($\nu_{C=O}$ ester), 1635 (amide I), 1535 (amide II); ^{1}H NMR ($CDCl_3$, 55 °C): δ 0.87 (broad, CH_3, 3H), 1.26 (broad, CH_2, 14H), 1.54 (broad, CH_3 and CH_2, 5H), 4.10 (broad, CH_2, 2H), 4.52 (broad, CH, 1H), 4.9−7.7 (broad, aromatic, 4H), 8.0−9.1 (broad, NH, 1H); $[\alpha]^{25}_D$ +1062° (*c* 0.05, chloroform). Anal. Calcd (%) for $(C_{21}H_{30}N_2O_3)_n$: C, 70.36; H, 8.44; N, 7.81. Found: C, 70.36; H, 8.32; N, 7.64.

Spectroscopic data of poly-D-1(+): IR (KBr, cm^{-1}): 3277 (ν_{N-H}), 1751 ($\nu_{C=O}$ ester), 1635 (amide I), 1535 (amide II); ^1H NMR ($CDCl_3$, 55 °C): δ 0.86 (broad, CH_3, 3H), 1.26 (broad, CH_2, 14H), 1.53 (broad, CH_3 and CH_2, 5H), 4.10 (broad, CH_2, 2H), 4.52 (broad, CH, 1H), 4.9−7.8 (broad, aromatic, 4H), 7.9−8.9 (broad, NH, 1H); $[\alpha]^{25}_D$ +1487° (*c* 0.1, chloroform). Anal. Calcd (%) for $(C_{21}H_{30}N_2O_3)_n$: C, 70.36; H, 8.44; N, 7.81. Found: C, 70.00; H, 8.62; N, 7.42.

In the same way, poly-L-**1**$_{50}$ ([**1**]/[**2**] = 50) and poly-L-**1**$_{200}$ ([**1**]/[**2**] = 200) were prepared by the polymerization of L-**1** with **2** in THF at 55 °C for 20 h, and poly-L-**1**$_{50}$(−) and poly-L-**1**$_{200}$(−) were obtained as the acetone-insoluble part from the poly-L-**1**$_{50}$ and poly-L-**1**$_{200}$, respectively.

Spectroscopic data of poly-L-1$_{50}$: IR (KBr, cm^{-1}): 3281 (ν_{N-H}), 1748 ($\nu_{C=O}$ ester), 1636 (amide I), 1536 (amide II); ^1H NMR ($CDCl_3$, 55 °C): δ 0.89 (broad, CH_3, 3H), 1.26 (broad, CH_2, 14H), 1.56 (broad, CH_3 and CH_2, 5H), 4.12 (broad, CH_2, 2H), 4.53 (broad, CH, 1H), 4.7−7.7 (broad, aromatic, 4H), 7.9−9.1 (broad, NH, 1H); $[\alpha]^{25}_D$ −876° (*c* 0.1, chloroform). Anal. Calcd (%) for $(C_{21}H_{30}N_2O_3)_n$: C, 70.36; H, 8.44; N, 7.81. Found: C, 70.13; H, 8.28; N, 7.99.

Spectroscopic data of poly-L-1$_{50}$(−): IR (KBr, cm^{-1}): 3279 (ν_{N-H}), 1750 ($\nu_{C=O}$ ester), 1634 (amide I), 1535 (amide II); ^1H NMR ($CDCl_3$, 55 °C): δ 0.88 (broad, CH_3, 3H), 1.26 (broad, CH_2, 14H), 1.54 (broad, CH_3 and CH_2, 5H), 4.11 (broad, CH_2, 2H), 4.52 (broad, CH, 1H), 4.9−7.7 (broad, aromatic, 4H), 7.9−9.0 (broad, NH, 1H); $[\alpha]^{25}_D$ −1659° (*c* 0.1, chloroform). Anal. Calcd (%) for $(C_{21}H_{30}N_2O_3)_n$: C, 70.36; H, 8.44; N, 7.81. Found: C, 70.38; H, 8.50; N, 7.72.

Spectroscopic data of poly-L-1$_{200}$: IR (KBr, cm^{-1}): 3276 (ν_{N-H}), 1751 ($\nu_{C=O}$ ester), 1635 (amide I), 1535 (amide II); ^1H NMR ($CDCl_3$, 55 °C): δ 0.86 (broad, CH_3, 3H), 1.24 (broad, CH_2, 14H), 1.53 (broad, CH_3 and CH_2, 5H), 4.07 (broad, CH_2, 2H), 4.47 (broad, CH, 1H), 4.8−7.7 (broad, aromatic, 4H), 7.9−9.0 (broad, NH, 1H); $[\alpha]^{25}_D$ −1083° (*c* 0.1, chloroform). Anal. Calcd (%) for $(C_{21}H_{30}N_2O_3)_n$: C, 70.36; H, 8.44; N, 7.81. Found: C, 70.09; H, 8.32; N, 7.63.

Spectroscopic data of poly-L-1$_{200}$(−): IR (KBr, cm^{-1}): 3277 (ν_{N-H}), 1740 ($\nu_{C=O}$ ester), 1635 (amide I), 1533 (amide II); ^1H NMR ($CDCl_3$, 55 °C): δ 0.87 (broad, CH_3, 3H), 1.24 (broad, CH_2, 14H), 1.53 (broad, CH_3 and CH_2, 5H), 4.08 (broad, CH_2, 2H), 4.51 (broad, CH, 1H), 4.8−7.7 (broad, aromatic, 4H), 7.9−9.0 (broad, NH, 1H); $[\alpha]^{25}_D$ −1714° (*c* 0.1, chloroform). Anal. Calcd (%) for $(C_{21}H_{30}N_2O_3)_n$: C, 70.36; H, 8.44; N, 7.81. Found: C, 70.34; H, 8.36; N, 7.70.

WAXD Measurements. The oriented helical poly-L-**1**(−) and poly-L-**1**(+) films (ca. 20 μm thickness) for the X-ray analyses were prepared from concentrated LC benzene solutions in an electric field of 6000 V/cm. The WAXD patterns of the oriented poly-L-**1**(−) and poly-L-**1**(+) films with different ranges of sensitivities to show both the strong and weak reflections (Figure S2), where the main layer lines have been indicated and the indices of the reflections are labeled, exhibit diffuse equatorial reflections, and several meridional and off-meridional reflections on the layer lines, although the only broad reflections were observed in the diffraction pattern of poly-L-**1**(+) probably due to its relatively low molecular weight. The reflections in the diffraction patterns of poly-L-**1**(−) and poly-L-**1**(+) can be properly indexed with hexagonal lattices; a = 26.78 Å, c = 13.05 Å, and a = 26.45 Å, c = 13.20 Å, respectively. The spacings and mirror indices of the reflections are listed in Table S1. Although we could not observe a meridional reflection on the 15th layer line (0.87 Å) even when the X-ray measurements were performed using a cylindrical camera with the samples tilted ca. 62° normal to the beam, the most probable structure of the helical poly-L-**1**(−) and poly-L-**1**(+) can be proposed to be a 15/4 helix by considering the layer line intensities observed in the diffraction patterns and the density measurement[14] and calculation results.

SAXS Measurements. The oriented helical poly-L-**1**(−), poly-D-**1**(+), and poly-L-**1**$_{50}$(−) films for the SAXS measurements were prepared by gradual solvent evaporation of a concentrated LC chloroform solution of each polymer (initial concentration: ca. 20 wt %) in a borosilicate glass capillary tube in a high magnetic field (11.75 T) using a Varian AS500 NMR instrument, after the polymers had been treated with CuCl in piperidine to eliminate the Pd residues at the polymer ends, followed by SEC fractionation. We noted that the smectic layer reflections could not be observed for the magnetic-oriented polymers bearing the terminal Pd residues prepared under the identical conditions; the reason is not clear, but probably due to the high atomic scattering factor of the Pd metals at the polymer ends.

A typical procedure for the elimination reaction is described below (see Scheme 1). To a solution of poly-L-**1**(−) (41 mg) in piperidine (4 mL) was added a solution of CuCl in piperidine (28.8 mM, 50 μL; 2 equiv to the polymer) at ambient temperature. The mixture was then stirred at 120 °C under a dry argon atmosphere. After 9 h, the resulting polymer was precipitated in a large amount of acetonitrile, collected by filtration, and washed with acetonitrile. The polymer was then dissolved in a small amount of chloroform and precipitated in acetonitrile which was repeated a second time. The obtained polymer had a broad polydispersity (M_w/M_n = 1.20), and the polymer was fractionated by SEC using THF containing 0.1 wt % tetra-*n*-butylammonium bromide as the eluent, yielding poly-L-**1**(−) with a narrow polydispersity (25 mg, 61% yield, $M_n = 6.75 \times 10^4$, M_w/M_n = 1.04, $\Delta\epsilon_{364}$ = −21.8) after being purified by reprecipitation and dried in vacuo at ambient temperature for 10 h. In the same way, the Pd-eliminated poly-L-**1**$_{50}$(−) ($M_n = 2.83 \times 10^4$, M_w/M_n = 1.03, $\Delta\epsilon_{364}$ = −19.9) and poly-D-**1**(+) ($M_n = 5.13 \times 10^4$, M_w/M_n = 1.03, $\Delta\epsilon_{364}$ = +21.6) were prepared, and these samples were used for the SR-SAXS measurements. The resulting Pd-eliminated polymers gave almost identical CD, absorption, and NMR spectra to those of the original polymers, although their molecular weights and MWDs were slightly changed. These results suggest that the Pd elimination procedure did not cause a substantial change of the helical structures of the original polymers.

SEC-MALS Measurements. The SEC-MALS measurements were carried out with THF containing 0.1 wt % tetra-*n*-butylammonium bromide used as the eluent at the flow rate of 0.5 mL/min. A standard polystyrene (M_w = 30500 (Polymer Laboratories, Shropshire, U.K.)) was used to calculate the device constants, such as the interdetector delay, interdetector band broadening, and light-scattering detector normalization. Poly-L-**1**(−) and poly-L-**1**(+) were completely dissolved in the eluent at the concentration of 0.1−0.2% (wt/vol) under gentle stirring for 1−2 h before injection. The evaluations of the molecular weights were accomplished using ASTRA V software (version 5.1.3.0). The dn/dc values of poly-L-**1**(−) and poly-L-**1**(+) in the eluent used for the evaluations were 0.1369 and 0.1367 mL/g, respectively.

AFM Measurements. Stock solutions of poly-L-**1**, poly-L-**1**(+), poly-L-**1**(−), poly-D-**1**(+), and poly-L-**1**$_{200}$(−) in dry benzene or THF (0.015 or 0.02 mg/mL) were prepared. Samples for the AFM measurements were prepared by casting 20 μL aliquots of the stock solutions of the polymers. The casting was done at room temperature on freshly cleaved HOPG under benzene or THF vapor atmospheres. After the polymers had been deposited on the HOPG, the HOPG substrates were further exposed to benzene or THF vapors for 12 or 2 h, respectively, and then the substrates were dried under vacuum for 2 h according to the reported procedure.[8,16] The organic solvent vapors were prepared by putting 1 mL of benzene or THF into a 2-mL flask that was inside a 50-mL flask, and the HOPG substrates were then placed in the 50-mL flask. The typical settings of the AFM for the high-magnification observations were as follows: amplitude 1.0−1.5 V, set point 0.9−1.4 V, scan rate 2.5 Hz. The Nanoscope image processing software was used for the image analysis.

Acknowledgment. We thank Professors A. Takano and Y. Matsushita (Nagoya University) for their help with the SR-SAXS measurements.

Supporting Information Available: Molecular modeling and calculations of helical structures of poly-L-**1**(+) and poly-L-**1**(−), SEC chromatograms and CD and UV−vis spectra of as-prepared poly-D-**1**, poly-D-**1**(+), and poly-D-**1**(−), WAXD patterns and lattice data of oriented poly-L-**1**(−) and poly-L-**1**(+) films, IR spectra of poly-L-**1**, poly-L-**1**(−), and poly-L-**1**(+) in chloroform, crystalline structure of L-**1**, AFM images of 2D self-assembled, as-prepared poly-L-**1**, poly-D-**1**(+), poly-L-**1**$(-)_{200}$, poly-L-**1**(−), and poly-L-**1**(+) on HOPG, SR-SAXS pattern of a magnetically oriented poly-L-**1**$(-)_{50}$. This material is available free of charge via the Internet at http://pubs.acs.org.

JA074627U